Axonal transport of herpes simplex virions to epidermal cells: Evidence for a specialized mode of virus transport and assembly

MARK E. T. PENFOLD*†, PATRICIA ARMATI†, AND ANTHONY L. CUNNINGHAM*‡

*Virology Department, Centre for Infectious Diseases and Microbiology, Institute of Clinical Pathology and Medical Research, Westmead Hospital, 2145, and University of Sydney, 2001, New South Wales, Australia; and †School of Biological Sciences, University of Sydney, 2001, New South Wales, Australia

ABSTRACT   To examine the transmission of herpes simplex virus (HSV) from axon to epidermal cell, an *in vitro* model was constructed consisting of human fetal dorsal root ganglia cultured in the central chamber of a dual-chamber tissue culture system separated from autologous skin explants in an exterior chamber by concentric steel cylinders adhering to the substratum through silicon grease and agarose. Axons grew through the agarose viral diffusion barrier and terminated on epidermal cells in the exterior chamber. After inoculation of HSV onto dorsal root ganglia, anterograde axonal transport of glycoprotein and nucleocapsid antigen was observed by confocal microscopy to appear in exterior chamber axons within 12 h and in epidermal cells within 16 h, moving at 2–3 mm/h. Although both enveloped and unenveloped nucleocapsids were observed in the neuronal soma by transmission electron microscopy, only nucleocapsids were observed in the axons, closely associated with microtubules. Nodule formation at the surface of HSV-infected axons, becoming more dense at the axon terminus on epidermal cells, and patches of axolemmal HSV glycoprotein D expression were observed by scanning (immuno)electron microscopy, probably representing virus emerging from the axolemma. These findings strongly suggest a specialized mode of viral transport, assembly, and egress in sensory neurons: microtubule-associated intermediate-fast anterograde axonal transport of unenveloped nucleocapsids with separate transport of glycoproteins to the distal regions of the axon and assembly prior to virus emergence at the axon terminus.

Herpes simplex virus (HSV) initially infects epidermal cells of the natural human host or animal models, followed by entry into cutaneous sensory axonal twigs and retrograde axonal transport to the neural soma and nucleus. This results in acute ganglionitis and/or development of neuronal latency. Later intermittent viral reactivation, anterograde axonal transport, and transmission back to epidermal cells in the same or adjacent dermatomes may result in intermittent asymptomatic shedding of virus in saliva or genital secretions or in recurrent clinical lesions (1, 2). While most of these stages have been carefully studied (3, 4), there is little data on anterograde viral transport and transmission to epidermal cells.

These latter stages are important for two reasons. (*i*) In people infected with HSV, recurrent clinical lesions are much less common than asymptomatic shedding (1, 2), but this ratio is reversed during immunosuppression, reverting to normal when immunosuppressive drugs are withdrawn (5). These observations suggest that there is immune restriction of viral replication in the epidermis in the immunocompetent host, despite continuing axonal transport of HSV and asymptomatic shedding. An *in vitro* system is needed to examine the effects of immune factors, including cytokines, on HSV

transmission from axon to epidermal cell and subsequent viral replication.

(*ii*) The transport of HSV-1 from neuronal soma via axons to epidermal cells may be specialized. Ultrastructural observations of HSV-1 replication and egress in cultured cell lines showed that virus buds from the inner nuclear membrane into the perinuclear cisterna. The mechanism of envelopment of HSV and transport between the perinuclear cisterna and the cell surface remains controversial. One hypothesis is that enveloped virus is incorporated into vesicles and transported to the extracellular environment via the endoplasmic reticulum and Golgi apparatus (4, 6, 7). However, the presence of unenveloped nucleocapsids within the cytoplasm and beneath the cytoplasmic membrane has been interpreted to represent a second "cytoplasmic envelopment" pathway of viral egress where HSV is deenveloped at the outer nuclear membrane, reenveloped by budding into cytoplasmic vesicles, and released at the cell surface by exocytosis (8, 9). Some recent data suggest this pathway may be abortive (6, 10). However, due to the unique anatomy of sensory neurons, axonal transport of virions over distances of 10–100 cm and egress to epidermal cells may involve modifications of stages of these transport pathways.

Therefore, we developed a unique chamber system in which the neural soma in the central chamber and the axonal termini of individual human neurons plus autologous epidermal cells in the exterior chamber are maintained in separate environments. Previous two-chamber *in vitro* systems employed rat neural tissue alone (11). Our *in vitro* model allowed inoculation of sensory neurons in the central chamber and observation of anterograde transport of HSV-1 in axons and transmission from axon termini to epidermal cells in the exterior chamber.

MATERIALS AND METHODS

Viruses, Cell Lines, and Antibodies. *Virus.* Clinical isolates of HSV-1 (WM1 and WM2) were passaged six times in Hep-2 cells to a titer of 10^5–10^6 TCID$_{50}$ (tissue culture 50% infective dose) in human endothelial fibroblasts (HEFs) and typed with fluorescein-conjugated anti-glycoprotein C (gC) monoclonal antibodies.

Cell lines. HSV-1 was cultivated in HEFs (MRC-5) or Hep-2 cells (Commonwealth Serum Laboratories, Parkville, Australia).

Monoclonal antibodies. Mouse monoclonal antibodies that recognized purified human brain neurofilament (BioGenex Laboratories, San Ramon, CA) and the β subunit of purified

rat brain tubulin (Sigma) were diluted 1:200. Mouse mono-clonal antibodies to HSV-1 glycoprotein D (gD) (Cymbus Bioscientific, Southampton, U.K.) and gC (Biosoft, Paris, France, and Syva, San Jose, CA) were diluted 1:50. Rabbit polyclonal antibody to HSV-1 nucleocapsid protein 1 (NC1 or VP5) (12) was kindly supplied by G. Cohen and R. Eisenberg (University of Pennsylvania, Philadelphia) and diluted 1:2000.

Preparation of Human Fetal Tissue. Human fetal thoracic, sacral, and cervical dorsal root ganglia (DRGs) and cranial skin were dissected from fetuses 15–20 weeks after menstruation, obtained from therapeutic terminations after informed consent, and carefully cleaned of connective tissue. They were washed in 70% ethanol for 30–60 s and rinsed twice in Hanks' calcium/magnesium-free saline. Dermal and subcutaneous tissue was removed from skin and cut into 1-mm^3 explants (13).

Establishment of the Dual Chamber Neuron–Epidermal Cell System. Extracellular matrix was produced on glass or Lux plastic coverslips in cluster well plates by lysis of a confluent HEF monolayer with 0.5% Triton X-100 in phosphate-buffered saline (PBS) (13). Two concentric stainless steel rings with two radial grooves on their lower face were fixed to the center of the coverslip with silicon grease and liquid agarose [2% (vol/wt) in double-distilled water] pipetted between the rings. Two DRGs were added to each central chamber and two skin explants were added to each exterior chamber. Outgrowth of epidermal cells occurred over 2 weeks (13), in medium containing nerve growth factor at 30 ng/liter. DRG neurons were maintained in D-valine medium (Commonwealth Serum Laboratories) containing 2 mM glutamine, D-glucose (5.12 g/liter), nerve growth factor (20 ng/liter), and Monomed A (50 ml/liter) (Commonwealth Serum Laboratories).

Confocal Laser Scanning Microscopy (CLSM). Cultures on glass coverslips for CLSM were fixed with 25% (vol/vol) glacial acetic acid in 95% methanol for 10 min at room temperature. Nonspecific binding of antibodies was blocked by incubation for 20 min with 100 μl of 5% (vol/vol) normal goat serum. Anti-gC monoclonal antibody, anti-NC1 polyclonal antibody, or antibody diluent as control at 100 μl was applied, washed three times in PBS, replaced with 100 μl of 10-nm colloidal gold-conjugated goat anti-mouse or anti-rabbit IgG (Amersham) diluted 1:50, and washed three times in PBS. Anti-neurofilament or anti-β-tubulin antibodies and fluorescein isothiocyanate-conjugated goat anti-mouse IgG diluted 1:100 (Tago) were applied similarly. Diluents were PBS plus 0.1% bovine serum albumin. Antibody incubation times were 1 h. Gold label was silver-enhanced for 4 min at 22°C (Amersham). By using the CLSM, mounted specimens were optically sectioned into eight segments, each segment was scanned five times for fluorescence, and the images were averaged. The same segments were rescanned in reflection mode and coplanar images were superimposed.

Scanning Immunoelectron Microscopy (SIEM) and Scanning Electron Microscopy (SEM). Cultures on glass coverslips for SIEM were washed with Sorenson's buffer, fixed with 4% (wt/vol) paraformaldehyde in Sorenson's buffer, incubated with 100 μl of anti-gD antibody, washed three times in PBS, incubated with 100 μl of 10-nm colloidal-gold-conjugated goat anti-mouse IgG (Amersham) diluted 1:50, and washed three times in PBS. Cultures for SEM were washed with 0.1 M Mops (pH 7.4), fixed for 20 min in Karnovsky's fixative, dehydrated through a graded alcohol series (14), critical-point-dried, sputter-coated with 2-nm platinum, and observed with a JEOL 6400F field emission scanning electron microscope. Gold label was detected using back-scattered electron imaging.

Transmission Electron Microscopy (TEM). Cultures on plastic coverslips were washed gently with 0.1% Mops (pH

7.4) and fixed for 1 h with Karnovsky's fixative. Cells were postfixed for 1 h in aqueous buffered 2% (wt/vol) OsO₄ followed by aqueous 2% (wt/vol) uranyl acetate, dehydrated through a graded alcohol series (14), and embedded in Spurr resin.

Thin sections were cut on an Ultracut E ultramicrotome, placed on copper grids, and poststained with aqueous 2% uranyl acetate in 50% ethanol and Reynold's lead citrate solution. Sections were examined using a Phillips 201 transmission electron microscope at 60 kV.

RESULTS

Principle of the *in Vitro* Neuron–Epidermal Cell Model. By using modified Campenot chambers (15), human fetal epidermis and spinal ganglia were cultured in separate annular chambers in plastic cluster wells. The tissues and growth medium were separated from each other by a semiimpervious barrier consisting of two concentric stainless steel rings cemented to extracellular matrix-coated coverslips in the cluster well by silicon grease and agarose.

The silicone grease/agarose barrier was shown to be impervious to HSV-1 by inoculating vacant central chambers and assaying for HSV in supernatants and fibroblasts close to the ring in the exterior chamber by cocultivation with HEF and immunofluorescence with anti-gC monoclonal antibody, respectively, up to 72 h later.

Interaction of Neurons and Epidermal Cells in the Dual-Chamber System (Fig. 1). In the central chamber, growth of axons from DRGs commenced within 24 h, progressively forming fascicles and extending randomly from the explant. Outgrowth of Schwann cells and fibroblasts was minimal. By 6–8 days *in vitro*, fascicles penetrated the agarose barrier and entered the exterior chamber, where they branched into individual axons. These axons grew past occasional peripheral fibroblasts into the multilayer of epidermal cells that spread radially from skin explants. After 7–10 days of culture, these cells had formed stratified multilayers with epidermal keratinocytes resting on dermal fibroblasts, closely mimicking the structure of developing human fetal skin *in vivo* (13, 16).

Detection of Axonal Transport of HSV and Transmission to Epidermal Cells by CLSM (Fig. 2). To examine axonal transport of HSV-1 within the model, DRGs in the central chamber were inoculated with 100 TCID₅₀ of HSV-1. In infected cultures, there was a minor cytopathic effect in fibroblasts and Schwann cells in the central chamber within the first 48 h. However, there was no obvious alteration in neuronal morphology.

For CLSM, cultures were dual stained with either fluorescein-labeled neurofilament or β-tubulin antibodies and with either gold-labeled gC or NC1 antibodies. Nine hours after infection of the central chamber, intense staining for gC or NC1 was observed in the DRG and 70–80% of axons within the central chamber. In contrast, axons and epidermal cells in the exterior chamber remained unstained as did cells in control cultures. gC was first observed in distal regions of axons within the exterior chamber 12 h after inoculation. Viral antigen was observed in axons that terminated on or prior to epidermal cells. By 16 h, axons in contact with epidermal cells showed infection and there was scattered associated staining of epidermal cells (Fig. 2). As axons had an average length of 9 mm, the viral antigen was calculated to move at 2–3 mm/h. Positive staining spread from foci of neuro–epidermal contact and became more widespread in the exterior epidermal cells over the next 48 h (Table 1). Optical sectioning of axons indicated HSV-1 gC and NC1 were concentrated predominantly in the central regions of axons and were closely associated with staining for β-tubulin in microtubules (data not shown).
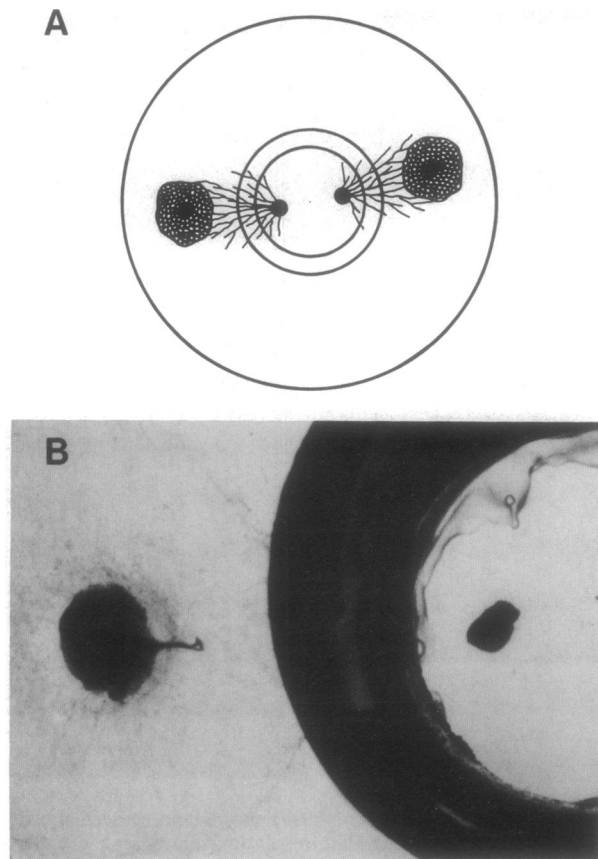
Microbiology: Penfold *et al.*

Proc. Natl. Acad. Sci. USA 91 (1994)   6531

FIG. 1. Representation of dual cell culture chamber. (*A*) Diagram of the chamber system shows neurites extending from central ganglia, penetrating the agarose barrier, and interacting with exterior epidermal cell multilayers. (*B*) Photomicrograph of a cluster well showing the position of the two rings and agarose barrier. The central well contains two DRGs. The outer annular chamber contains the skin explants surrounded by epidermal cell outgrowths after 14 days in culture.

Ultrastructural Morphology of HSV-1 During Anterograde Axonal Transport Examined by TEM.

To examine the mechanisms of axonal transport of HSV-1, cultures were inoculated with HSV-1 in (*i*) the exterior chamber (without epidermal cells) to examine retrograde transport or (*ii*) the central chamber to examine anterograde transport.
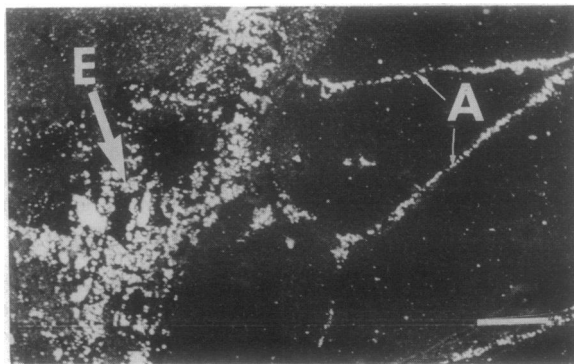

FIG. 2. CLSM of axons from DRG neurons interacting with epidermal cells 24 h after viral inoculation of DRGs. Cultures were stained with anti-gC1 or anti-NC1 monoclonal antibodies and gold-labeled. Viral antigen is seen as small bright granules in axonal fasicles (A) and the cytoplasm of infected epidermal cells (E). (Bar = 16 μm.) No intraaxonal or intraepidermal staining was observed when primary antibody was omitted.

Table 1. Appearance of viral nucleocapsid and gC antigen (observed by confocal microscopy) in regions of the chamber after inoculation of the central chamber with HSV-1

Time after inoculation, h	Region examined			
	Central DRG	Interior axon	Exterior axon	Epidermal cell
0	−	−	−	−
9	+	+	−	−
12	+ +	+ +	+	−
16	+ +	+ +	+ +	+
20	+ +	+ +	+ +	+
24	+ + +	+ + +	+ + +	+ +
48	+ + +	+ + +	+ + +	+ + +

−, Negative; +, weakly positive; + +, strongly positive; + + +, widespread infection.

To study anterograde transport, cultures were fixed at 0, 4, 16, 24, or 48 h and sectioned through distal and proximal regions of axons and the central region of the DRG explant. Sections through the proximal axons demonstrated unenveloped nucleocapsids identical to those observed in retrograde transport in humans (data not shown) and rats (17). These were also occasionally seen in the neuronal soma (Table 2). No nucleocapsids were observed in proximal axons 4 h after inoculation. After 16 h, nucleocapsids were observed in distal regions of axons and at 24 and 48 h within exterior-chamber epidermal cells. Nucleocapsids were more easily detected in the proximal regions of axons in the central chamber (>200 in 100 sections) than in distal axons in the outer chamber (12 in 90 sections) due to differences in the size and number of fascicles in each section. In the central chamber, 20–30 fasicles, each containing 8–12 axons, were present in each section, whereas in the outer chamber, there were 10–12 fasicles per section, each fasicle containing 2–4 axons. As with retrograde transport, nucleocapsids appeared to be closely associated with microtubules during anterograde transport. Enveloped virus enclosed within cytoplasmic membranes was observed in the neural soma more frequently than unenveloped nucleocapsids (Fig. 3 *Lower* and Table 2). Occasionally, the electron-dense core of virions and nucleocapsids was missing (data not shown). No enveloped virus was seen in proximal or distal regions of axons. The detection of no enveloped virions but >200 and 12 nucleocapsids in the proximal and distal regions of axons, respectively, compared with a ratio of 4 in the neural soma, is highly significant ($P <$ 0.0001, Fisher's exact test).

Detection of HSV-Specific Nodules or Axon Terminals by SEM.

To further characterize neuro–epidermal transmission of HSV-1, the interaction of axons and epidermal cells was examined by high-resolution SEM and showed axons terminating on epidermal cells (Fig. 4). In HSV-1-infected cultures, multiple nodules of 100–120 nm were observed on some terminals that themselves were only 150–200 nm in diameter (Fig. 5A). Similar nodules were also observed on preterminal regions of axons but were much more sparse.

Table 2. Summary of observations of anterograde transport of HSV-1 from transmission electron microscopic sections

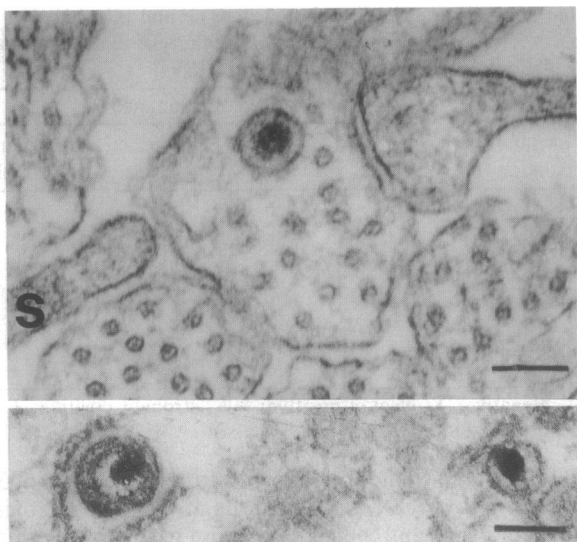| Parameter	Neural soma	Proximal region of axon	Distal region of axon
Specimens, no.	10	10	6
Sections observed per specimen, no.	10	10	15
Sections with virions, no.	8	80	10
Enveloped virions, no.	20	0	0
Unenveloped nucleocapsids, no.	5	>200	12

FIG. 3. TEM of intraneural viral particles. (*Upper*) A transversely sectioned fascicle in the outer chamber shows an unenveloped nucleocapsid in close proximity to microtubules in an axon, surrounded by other axons and a single Schwann cell process (S). Cells were fixed 16 h after inoculation of HSV into the central chamber. (Bar = 100 nm.) (*Lower*) Enveloped virus within a cytoplasmic vesicle and unenveloped nucleocapsids in the cytoplasm of the neuronal soma fixed 24 h after HSV inoculation.

Nodules were not seen in 0-h or uninfected controls but became more numerous at 16–24 h after inoculation. The size and shape of these nodules were similar to those observed in HSV-1-infected Hep-2 cells 24–48 h after inoculation (data not shown). gD was demonstrated on the surface of similar nodules by silver-enhanced immunogold staining and SIEM (Fig. 5*B*).

DISCUSSION

Little is known about the processes that follow the reactivation of HSV-1 in the neuronal soma. No animal model has yet provided an effective or reliable tool for the elucidation of the mechanisms involved in anterograde axonal transport and neuronal–epidermal transmission, probably due to difficulties in visualizing these events in the intact animal. There may also be differences in this part of the viral life cycle between human and animal hosts (4, 18–20).

Hence, in this paper, we present a model utilizing autologous human tissue *in vitro* that allowed close observation of these events. In this model, DRG neurons in the central well were separated from skin explants of epidermal cells overlying dermal fibroblast cells in the exterior well by an agarose

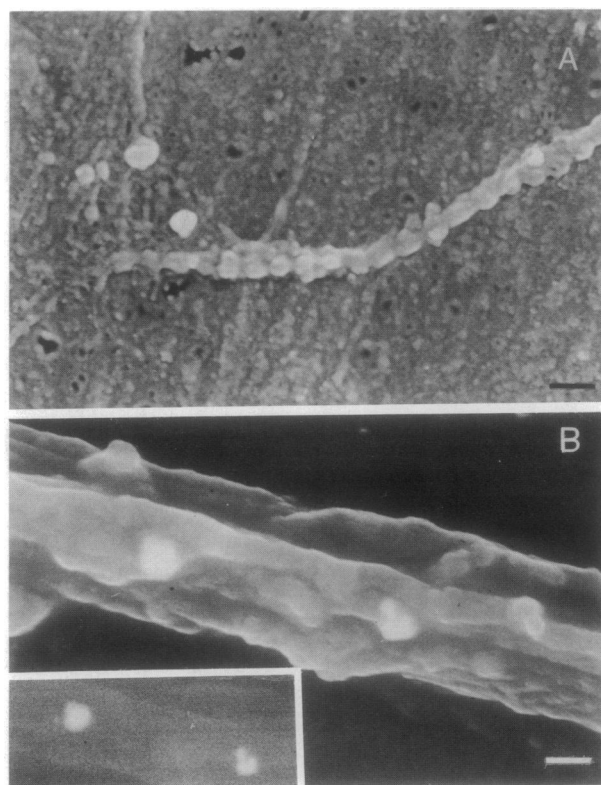FIG. 4. SEM of distal axons impinging on a stratified epidermal keratinocyte in the exterior chamber.

FIG. 5. SEM of HSV-1-infected neurons and epidermal cells in the exterior chamber. (*A*) High-resolution micrograph of an axon terminal showing multiple nodules (100–120 nm in diameter) and the underlying epidermal cell. Nodules were not observed in uninfected or 0-h control cultures. (*B*) Secondary electron image of a distal fascicle showing nodules labeled with gold-conjugated anti-gD1 monoclonal antibody in a culture fixed for SIEM (size of the nodules is exaggerated by silver enhancement). No staining was observed with control irrelevant monoclonal antibody. (Bar = 200 nm.) (*Inset*) Back-scattered electron image of the section in *B* demonstrates localization of expression of HSV-1 gD on the surface of axonal buds.

barrier that was impervious to viral diffusion. Axons from the central chamber grew through this barrier, bypassed sparse outlying fibroblasts, and terminated on the superficial epidermal cells in the exterior well. The mechanism for the attraction of the neuronal growth cone to epidermal cells, perhaps via keratinocyte secretion of nerve growth factor (21), is one of several neurobiological questions that could be addressed using this model.

Simpler two-chamber models, without skin explants and using a silicon diffusion barrier, have been used to show that retrograde transport of HSV-1 unenveloped nucleocapsids in rat sensory neurons was mediated by microtubules and was rapid (3–5 mm/h) consistent with experimental findings in whole animals (18, 19). In the present study retrograde transport of unenveloped HSV-1 nucleocapsids from human axons in the exterior to those in the central chamber was also rapid (3 mm/h, data not shown), probably by a similar mechanism.

In cultures inoculated with HSV-1 in the central chamber to investigate anterograde viral transport, enveloped virions within vesicles in the cytoplasm of the neuronal soma were observed, complementing similar observations of human fetal neurons (without axonal extensions) *in vitro* (22), rat neurons *in vitro* (11), and mouse nerve *in vivo* (20). This suggests that virus assembly in and egress from the soma may involve enveloped virus in pathways similar to those observed in cultured cell lines. However, our findings of only unenveloped nucleocapsids in axons extending to epidermal cells but both enveloped and unenveloped nucleocapsids in

Microbiology: Penfold *et al.*

Proc. Natl. Acad. Sci. USA 91 (1994) 6533

the cytoplasm of the soma support the hypothesis that there are marked differences in the pathways of transport, assembly, and egress of HSV-1 in the soma and axons of human neurons:

(*i*) Conventional assembly and transport of enveloped virions within vesicles to the cytoplasmic membrane, similar to that observed in cultured cell lines, may occur over short distances within the neuronal soma by either or both of the two hypothetical pathways (4, 6–10). This may result in infection of neighboring neurons or support cells.

(*ii*) Separate anterograde transport of unenveloped nucleocapsids and viral glycoprotein may occur within axons resulting in assembly at a distal site. This transport is probably microtubule-facilitated and may follow deenvelopment of enveloped virions at the outer lamella of the nuclear membrane prior to axonal transport of nucleocapsids, thus sharing some steps with the "cytoplasmic envelopment" pathway (8, 9).

This hypothesis is further supported by our finding that anterograde axonal transport of nucleocapsids and glycoproteins was rapid whereas transport of enveloped virus through the endoplasmic reticular would be relatively slow. Association of nucleocapsids with axonal microtubules was also strongly suggested by the relatively rapid velocity of transport (2–4 mm/h or 50–100 mm/day), which is similar to the well-defined intermediate to fast microtubule-associated axonal transport of organelles, neurotransmitters, and proteins (3–17 mm/h) (23, 24) and the proven microtubule-associated retrograde transport of nucleocapsids in rat axons (17). Close contact is highly likely between nucleocapsids that are 80–100 nm in diameter and microtubules in distal axons that are 70–100 nm apart (see Fig. 3). Our hypothesis could explain retention of the two pathways of viral transport, assembly within infected cell lines (6–10), and differences in their relative importance in different cell types.

Alternative interpretations of the marked predominance of unenveloped nucleocapsids in distal axons in static TEM images could be that deenveloped virions were transported distally immediately after virus entry in the central chamber or represent reinfection with progeny virions (10). However, the kinetics of neuronal expression of HSV-1 glycoprotein and capsid antigens, their anterograde axonal transport observed by confocal microscopy, and the presence of only unenveloped nucleocapsids in axons support the hypothesis that this is indeed the main method of axonal transport. Hence viral glycoproteins must be transported separately from nucleocapsids, probably within the neuritic transport vehicles commonly observed within axons, analogous to the transport of endogenous neuronal proteins (23). This hypothesis should be tested by future studies using transmission immunoelectron microscopy.

Intermediate-to-fast translocation of organelles, neurotransmitters, and proteins along axonal microtubules is associated with the cellular proteins, kinesin and a cytoplasmic dynein (MAP-IC), which produce movement in the anterograde and retrograde directions, respectively (23, 24). Separate interactions between different neuronal and viral tegument or capsid proteins should, therefore, facilitate such anterograde or retrograde transport of virions and could offer important therapeutic targets.

Sparse nodules along HSV-infected axons (with concentrations at the axon terminus) corresponded to focal patches of axonal membrane containing viral glycoproteins. These could be explained as viruses emerging by exocytosis or other mechanisms. It is unlikely that nodules are adherent virions released from other sites because of the kinetics of appearance of nodules, their distribution (concentration at the axon terminus), and the absence of patches of glycoprotein staining on adjacent fibroblasts that also have receptors for HSV. The mechanism for the marked increase in density of viral nodules in terminal axons is unknown but probably is determined by interactions with underlying epidermal cells. We have not yet directly observed HSV emerging from the axolemma facing the epidermal cell. Elucidation of the exact mechanism of HSV emergence from axons at all sites should require further exhaustive observations of serial sections by TEM.

1. Koutsky, L. A., Stevens, C. E., Holmes, K. K., Ashley, R. L., Kiviat, N. B., Critchlow, C. W. & Corey, L. (1992) *N. Engl. J. Med.* **326**, 1533–1539.
2. Douglas, R. G. & Couch, R. B. (1970) *N. Engl. J. Med.* **104**, 289–295.
3. Fraser, N. W. & Valyi-Nagy, T. (1993) *Microb. Pathog.* **15**, 83–91.
4. Roizman, B. & Sears, A. E. (1990) in *Fields Virology*, eds. Fields, B. N. & Knipe, D. M. (Raven, New York), pp. 1795–1842.
5. Rand, K., Rasmussen, L., Pollard, R., Arvin, A. & Merigan, T. (1976) *J. Immunol.* **296**, 1372–1377.
6. Baines, J. D., Ward, P. L., Campadelli Fiume, G. & Roizman, B. (1991) *J. Virol.* **65**, 6414–6424.
7. Johnson, D. C. & Spear, P. G. (1982) *J. Virol.* **43**, 1102–1112.
8. Nii, S., Morgan, C. & Rose, H. (1968) *J. Virol.* **2**, 517–536.
9. Nixon, F. J., Addison, C. & McLauchlan, J. (1992) *J. Gen. Virol.* **73**, 277–284.
10. Campadelli Fiume, G., Farabegoli, F., Di Gaeta, S. & Roizman, B. (1991) *J. Virol.* **65**, 1589–1595.
11. Lycke, E., Kristensson, K., Svennerholm, B., Vahlne, A. & Ziegler, R. (1984) *J. Gen. Virol.* **65**, 55–64.
12. Cohen, G. H., Ponce de Leon, M., Diggelmann, H., Lawrence, W. C., Vernon, S. K. & Eisenberg, R. J. (1980) *J. Virol.* **34**, 521–531.
13. Penfold, M. E., Armati, P. & Cunningham, A. L. (1992) *In Vitro Cell Dev. Biol.* **28A**, 223–226.
14. Glauert, A. M. (1974) *Practical Methods in Electron Microscopy: Part 1, Fixation, Dehydration and Embedding of Biological Specimens* (North-Holland, Amsterdam), Vol. 3, Part 1.
15. Campenot, R. B. (1977) *Proc. Natl. Acad. Sci. USA* **74**, 4516–4519.
16. Breathnach, A. (1971) *An Atlas of the Ultrastructure of Human Skin* (Churchhill, London).
17. Kristensson, K., Lycke, E., Roytta, M., Svennerholm, B. & Vahlne, A. (1986) *J. Gen. Virol.* **67**, 2023–2028.
18. Stanberry, L. R. (1986) *Prog. Med. Virol.* **33**, 61–77.
19. Wildy, P. (1967) *J. Hyg.* **65**, 173.
20. Hill, T. J., Field, H. J. & Roome, A. P. (1972) *J. Gen. Virol.* **15**, 233–235.
21. Di Marco, E., Marchisio, P. C., Bondanza, S., Franzi, A. T., Cancedda, R. & De Luca, M. (1991) *J. Biol. Chem.* **266**, 21718–21722.
22. Lycke, E., Hamark, B., Johansson, M., Krotochwil, A., Lycke, J. & Svennerholm, B. (1988) *Arch. Virol.* **101**, 87–104.
23. Ochs, S. & Brimijoin, W. S. (1993) in *Peripheral Neuropathy*, eds. Dyck, P. J., Thomas, P. K., Griffin, J. W., Low, P. A. & Podeslo, J. F. (Saunders, Philadelphia), 3rd Ed., pp. 331–360.
24. Vale, R. D., Schnapp, B. J., Mitchison, T., Steuer, E., Reese, T. S. & Sheetz, M. P. (1985) *Cell* **43**, 623–632.